pISSN 2384-1095
eISSN 2384-1109

iMRI 2020;24:132-140

https://doi.org/10.13104/imri.2020.24.3.132

iMRI
Investigative Magnetic Resonance Imaging

Comparison of Standard and Specialized Readings in Routine Practice for the Assessment of Extraprostatic Extension of Prostate Cancer on MRI after Biopsy

Sung Hee Shin, See Hyung Kim, Hunkyu Ryeom

Department of Radiology, School of Medicine, Kyungpook National University, Kyungpook National University Hospital, Daegu, Korea

Original Article

Received: August 12, 2019
Revised: October 24, 2019
Accepted: November 15, 2019

Correspondence to:
See Hyung Kim, M.D., Ph.D.
Department of Radiology, School of Medicine, Kyungpook National University, Kyungpook National University Hospital, 130 Dongdeok-ro, Jung-gu, Daegu 41944, Korea.
Tel. +82-53-200-5390
Fax. +82-53-422-2677
E-mail: kimseehyung72@outlook.kr

Purpose: To retrospectively determine whether specialized magnetic resonance imaging (MRI) reading performed by an experienced radiologist affected the successful assessment of extraprostatic extension (EPE) in the presence of biopsy-related hemorrhage after prostate biopsy.

Materials and Methods: Two hundred consecutive patients with biopsy-proven prostate cancer underwent MRI. General radiologist and subspecialized radiologist readings were unpaired and reviewed in random order by a radiologist who was blinded to patients' clinical details and histopathologic data. The extent of hemorrhage was assessed on T1-weighted (T1W) MRI using a 1-4 scale, and the likelihood of EPE was assessed for each of the four categories. Histopathologic specimens served as the reference standard. The area under the curve (AUC) of the standard reading was compared to that of the specialized reading.

Results: Post-biopsy hemorrhage was subjectively graded as ≥ 3 in 101 patients (50.5%) by standard reading, and in 100 patients (50.0%) by specialized reading. The standard and specialized readings disagreed for 40 (20.7%) of the patients (kappa [κ] = 0.35; 95% CI, 0.14-0.48). Of these, specialized reading was the correct interpretation for 21 patients (52.5%). The sensitivity (75% vs. 44%; P = 0.002) and area under the receiver operating characteristics (AUROC) (0.83 vs. 0.67; P = 0.008) of the specialized readings were significantly higher than those of the standard readings, while there was no significant difference in specificity (84% vs. 87%; P = 0.434).

Conclusion: The reinterpretation of MRI by experienced radiologists significantly improves the diagnosis of EPE in prostate cancer in the presence of post-biopsy hemorrhage.

Keywords: Prostatic neoplasms; Extraprostatic extension; Magnetic resonance imaging; Biopsy

INTRODUCTION

Magnetic resonance imaging (MRI) has emerged as one the most promising techniques for local staging of prostate cancer (1, 2). Evaluation of extraprostatic extension (EPE) is a crucial component of the staging process, because the choice of

treatment is directly affected by the distinction between organ-confined disease (T1 and T2 stages) and non-organ-confined disease (T3 and T4 stages) (3). The presence of EPE can affect the decision of whether to perform a nerve-sparing or nerve-sacrificing prostatectomy (4, 5). Preoperative knowledge about the presence and localization of EPE is likely to reduce the number of patients with positive surgical margins. However, biopsy-related hemorrhage is the most common complication and can prevent accurate staging of prostate cancer because most patients undergo prostate MRI after biopsy. Despite advances in MRI technology and improved spatial resolution, this problem still occurs. In previous studies, a delay of three weeks was recommended for hemorrhage resolution, and more recent studies suggest that a delay of eight weeks may be more beneficial (6-8). These delays may postpone treatment decisions.

Meanwhile, the accuracy of MRI for the assessment of EPE varies widely, with sensitivities and specificities ranging from 13-95% and 49-97%, respectively (9-11). To our knowledge, few studies have investigated how the assessment of EPE correlates with biopsy-related hemorrhage on MRI by using the Prostate Imaging Reporting and Data System (PI-RADS) V2. Also, although the use of MRI for determining EPE in newly diagnosed prostate cancer has increased in tertiary referral institutions, its diagnostic performance is highly dependent on the radiologist's experience.

Therefore, the purpose of our study was to retrospectively evaluate whether the second-opinion MRI readings by experienced radiologists affects the assessment of EPE after prostate biopsy.

MATERIALS AND METHODS

Patients

Our Institutional Review Board approved and issued a waiver of informed consent for this retrospective study. A search of institutional databases identified 282 consecutive men with a biopsy-proven diagnosis of prostate cancer who had undergone prostate MRI within 180 days prior to radical prostatectomy (RP) and standard step-section histopathologic maps between September 2015 to December 2018. Of these cases, 82 patients were then excluded for the following reasons: patient received hormones or radiation therapy before MRI (n = 45); MRI was performed with a 1.5-T scanner (n = 20); or poor MRI quality prevented the diagnostic assessment of EPE by one of two radiologic readers (n = 17). These exclusions resulted in a final cohort of 200 patients. In this cohort, the mean and SD of the interval between biopsy and MRI was 34 ± 23 days (median, 47.5 days; range, 6-154 days), and the mean and SD of the interval between MRI and prostatectomy was 30 ± 19 days (median, 23 days; range, 2-105 days; two patients had intervals greater than 60 days).

MRI Technique

MRI was performed with a 3-T MR imager (Achieva or Ingenia CX; Philips Healthcare, Best, the Netherlands) with a 32-channel phased-array surface coil (SENSE; Philips Healthcare). An intramuscular injection of 1 mg of glucagon was administered to suppress bowel peristalsis. The MRI acquisition parameters are summarized in Table 1.

After initial localizer images were obtained to determine the anatomic orientation of the prostate, T2-weighted (T2W) fast spin-echo images were obtained in 3 orthogonal planes. Spatial resolution was reduced in the sagittal plane to shorten acquisition time. T1W and T2W fast spin-echo

Table 1. MRI Parameters

Methods	Orientation	TR (ms)	TE (ms)	FOV (mm)	Matrix	Slice thickness (mm)	Number of slices	Acquisition time (second)
T2WI	Axial	4210	104	160 x 160	320 x 256	3	16	375
T2WI	Coronal	4000	104	150 x 150	320 x 256	3	15	302
T2WI	Sagittal	3500	96	180 x 180	256 x 204.8	3	14	117
T1WI	Axial	820	10	350 x 262.5	320 x 288	5	36	185
DWI	Axial	3500	75	340 x 168	170 x 170	4	16	175
DCE-MRI	Axial	4	1.3	280 x 227.6	256 x 230.4	2	30	305

DCE-MRI = dynamic contrast enhanced magnetic resonance imaging; DWI = diffusion weighted image; FOV = field of view; MRI = magnetic resonance imaging; T1WI = T1-weighted image; T2WI = T2-weighted image; TE = echo time; TR = repetition time

series covering the entire pelvis were acquired for lymph node detection and to detect hemorrhage in the prostate. Diffusion weighted (DW) images were acquired using 2D echo-planar imaging with 3 b values (0, 100 and 1000 s/mm^2) in 3 orthogonal directions. A 3D fast low-angle shot sequence was used to perform dynamic contrast enhanced magnetic resonance imaging (DCE-MRI). After 3 baseline acquisitions, gadobutrol (gadolinium chelate; Gadovist, Bayer, Germany) was administered as a bolus injection of 0.1 mmol/kg body weight at a rate of 2 mL/s, followed by a 20 mL flush of normal saline during a 10 s break before 21 post-contrast images were acquired with a temporal resolution of 12.9 s. In DCE-MRI, there is a 4-7 seconds lapse between spatial and temporal resolution of 4-7 seconds. Contrast agent distribution was observed for 4.5 min after injection. All axial images were identically angled along the prostate's longest axis, perpendicular to the urethra.

Histopathologic Analysis

RP specimens were fixed in 40% buffered formalin then serially sliced into horizontal sections at 4-6 mm thickness intervals using a step-by-step approach. If necessary, whole sections were divided into two to four blocks for processing. All tissues were paraffin-embedded and cut into sections with a thickness of four microns, and then stained with Hematoxylin and Eosin (12). All RP specimens at our institution are read by dedicated genitourinary pathologists (17 years of experience in genitourinary section) who determine the presence or absence of EPE for each patient using a standardized reporting template (13). These results were obtained from the histopathology report for each patient in the cohort.

The cancer foci were outlined, and the locations of EPE on each slide, final pathologic stage, and Gleason grade were documented.

Imaging Analysis

All cases were reviewed independently by two radiologists using a commercial workstation. The radiologists were aware that all patients underwent prostatectomy but were blinded to patient identity as well as further histological or clinical details.

For the purpose of this study, both the initial reports (standard reading) by radiologist 1 (abdominal imaging fellow with 2 years of experience) and the second-opinion reports (specialized reading) by radiologist 2 (subspecialized uroradiologist with 17 years of experience) were presented to a third radiologist with 15 years of experience in prostate MRI interpretation. All patient reports were unpaired and presented in random order to reduce bias by minimizing risk of identifying whether a report was the initial or second-opinion report.

During the first session, the radiologists only reviewed the axial T1W images for each patient and assigned a score to reflect the extent of hemorrhage within each sextant (peripheral or transition zone, and right or left base, mid-gland, or apex). The following scale was used: 1 = hemorrhage involving less than 25% of the sextant; 2 = hemorrhage involving 25-50% of the sextant; 3 = hemorrhage involving 50-75% of the sextant; 4 = hemorrhage involving greater than 75% of the sextant. The hemorrhage scores for each sextant were added to obtain a total hemorrhage score for each patient.

Next, as a part of every structured report and regardless of the PI-RADS V2 score, the reviewer was also asked to extract and interpret the information about the presence or absence of EPE provided and to assign each report to one of four categories. The four assessment categories were as follows: the radiology report states that there is no EPE; the radiology report states that there is a low-grade suspicion of EPE; the radiology report states that there is a high-grade suspicion of EPE; or the radiology report states that EPE is present.

The results from the standard reading and the second-opinion specialist reading were then compared to one another using the reference standard (i.e., the presence or absence of EPE on histopathologic analysis of the RP specimen). For statistical purposes, patients rated as high-grade suspicion of EPE or EPE present were grouped together as positive for the presence of EPE, whereas those with no EPE or low-grade suspicion of EPE were considered negative.

Statistical Analyses

The presence, location, and extent of post-biopsy hemorrhage were summarized with frequencies and percentages. Interreader agreement was assessed using weighted κ statistics and interpreted as follows: values of less than 0.20 were indicative of poor agreement; 0.20-0.40, fair agreement; 0.41-0.60, moderate agreement; 0.61-0.80, good agreement; and 0.81-1.00, very good agreement.

Nonparametric Receiver Operating Characteristics (ROC) analysis was performed using the histopathologic report as the reference standard to assess performance for the detection of EPE.

The AUC for the standard reading was compared with that of specialized reading using the nonparametric approach by DeLong et al. (14). The reports were then dichotomized as negative for EPE (no EPE or low-grade suspicion of EPE) or positive for EPE (high-grade suspicion of EPE or EPE present) based of the radiologists' interpretations, and measures of accuracy including sensitivity and specificity were assessed separately for the standard and specialized readings. Sensitivities and specificities were compared using the McNemar test. The simple κ statistic was used to assess agreement between dichotomized EPE status between the standard and specialized readings. The sensitivity was further compared between standard and specialized readings using both reading and technique as covariates. The relationship between EPE and total hemorrhage score was assessed on a patient-level basis using Pearson's correlation coefficient.

A P-value ≤ 0.05 was considered statistically significant.

Table 2. Patient Characteristics

Variable	Value
Age*	62 (50-77)
Prostate specific antigen (ng/d)*	8.2 (3.7-118.2)
Cancer volume (cm^3) *	2.52 (1.3-9.8)
Cancer lesion location	
Peripheral zone	185 (82.9)
Transition zone	38 (17.1)
Extraprostatic extension	
Presence	83 (41.5)
Absence	117 (58.5)
Pathological Stage	
T2a	16 (8.0)
T2b	2 (1.0)
T2c	99 (49.5)
T3a	62 (31.0)
T3b	19 (9.5)
T4	2 (1.0)
Extraprostatic extension per Gleason score	
≤ 3+3	8 (9.8)
3+4	16 (19.2)
4+3	21 (25.3)
≥ 4+4	38 (45.7)

Unless otherwise indicated, data are numbers, with percentages in parentheses.
*Data are the range.

Statistical analyses were performed using SAS version 9.2 (SAS Institute).

RESULTS

The median age of the study population at the time of RP, was 62 years (range, 50-77 years). A total of 233 cancer lesions were identified at histopathological assessment. Patients characteristics are described in Table 2.

The standard and specialized readings identified post-biopsy hemorrhage in the peripheral zone in 130 (65%) and 133 (66.5%) of the 200 patients, respectively. When present in the peripheral zone and/or transition zone, post-biopsy hemorrhage was subjectively graded as 3 and 4, respectively, in 83 patients (41.5%) and 18 patients (9.0%) by standard reading, and in 80 patients (40.0%) and 20 patients (10.0%) by specialized reading. Mean hemorrhage scores were 1.57 ± 1.23 and 1.43 ± 1.15, standard versus specialized. The interreader agreement for the extent of post-biopsy hemorrhage was good (κ = 0.80). The location of the post-biopsy hemorrhage according to each reading is summarized in Table 3.

The standard reading was frequently interpreted as no

Table 3. Presence and Extent of Post-biopsy Hemorrhage

Characteristic	Standard reading	Specialized reading
Extent of biopsy-related hemorrhage		
1	55 (27.5)	57 (28.5)
2	44 (22.0)	43 (21.5)
3	83 (41.5)	80 (40.0)
4	18 (9.0)	20 (10.0)
Number of sextants with biopsy-related hemorrhage		
Peripheral zone		
0 sextant	70 (35.0)	67 (33.5)
1-2 sextants	29 (14.5)	27 (13.5)
3-4 sextants	37 (18.5)	35 (17.5)
5-6 sextants	64 (32.0)	71 (35.5)
Transition zone		
0 sextant	137 (68.5)	134 (67.0)
1-2 sextants	45 (22.5)	52 (26.0)
3-4 sextants	15 (7.5)	13 (6.5)
5-6 sextants	3 (1.5)	1 (0.5)

Unless otherwise indicated, data are numbers, with percentages in parentheses.
Sextant location relates to right or left base, mid-gland, or apex.

EPE and low-grade suspicion of EPE, while the specialized reading was frequently interpreted as high-grade suspicion of EPE and EPE present. The interpretations of the standard and specialized readings were summarized in Table 4.

After dichotomization of the radiologist's interpretation classification, the standard and specialized readings disagreed for 40 (20.7%) of the 200 patients interpreted (κ = 0.35; 95% CI, 0.14-0.48). The specialized interpretation agreed with histopathology results (standard reference) in 21 (52.5%) of these 40 patients. The sensitivity of the specialized reading was significantly higher than that of standard reading (75% vs. 44%; P = 0.002), whereas there was no significant difference in specificity (87% vs. 84%; P = 0.434). The diagnostic performance for the assessment of EPE by standard and specialized readings is listed in Table 5.

The imaging technique (i.e., T1W plus T2W only vs. additional DW or DCE MRI) had no significant effect on the differences in sensitivity between the readings (P = 0.825).

Figure 1 shows the prevalence of EPE on histopathologic

Table 4. Classifications of Extraprostatic Extension Reported by Standard and Specialized Readings

EPE status	Standard reading	Specialized reading
No EPE	85 (42.5)	68 (34.0)
Low-grade suspicion of EPE	53 (26.5)	44 (22.0)
High-grade suspicion of EPE	38 (19.0)	52 (26.0)
EPE present	24 (12.0)	36 (18.0)

EPE = extraprostatic extension
Unless otherwise indicated, data are numbers, with percentages in parentheses.

Table 5. Diagnostic Performance of the Standard and Specialized Readings for the Assessment of Extraprostatic Extension

Variable	Standard reading	Specialized reading	P value
Sensitivity	44 (30-58)	75 (62-86)	0.002
Specificity	87 (74-95)	84 (70-93)	0.434
AUC	0.67 (0.56-0.79)	0.83 (0.72-0.91)	0.008

AUC = area under the curve
Unless otherwise indicated, data are percentage, with proportions of patients in parentheses and 95% CIs in brackets.

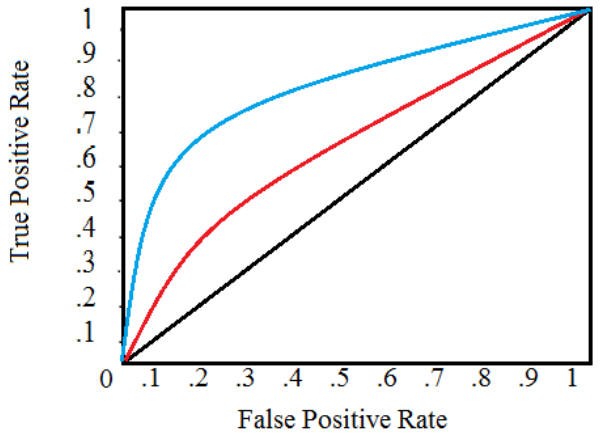

Fig. 2. ROC curves for the assessment of EPE with MRI. AUC with 95% CI is given for each set of reports. Black line denotes AUROC = 0.5. Blue curve = specialized reading and Red curve = standard reading.

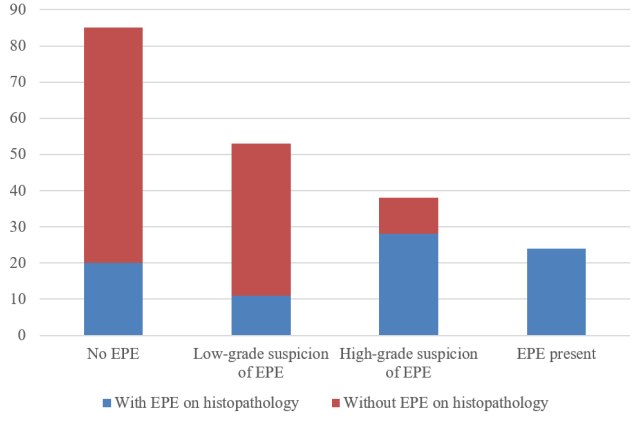

a

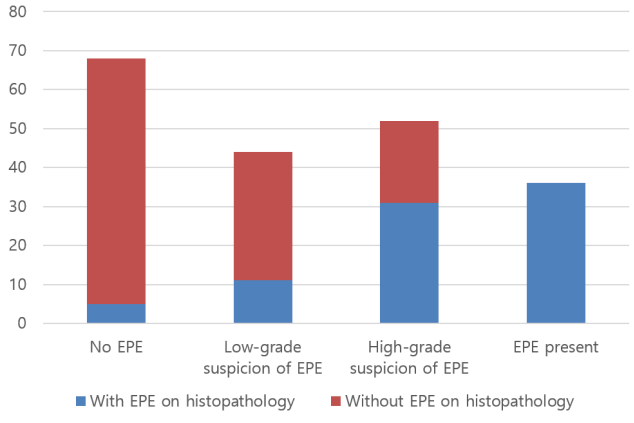

b

Fig. 1. Incidence of EPE on histopathologic analysis for each category in the classification system for standard readings (a) and specialized readings (b). Blue and red bars indicate proportions of patients with and without EPE on histopathology, respectively. Numbers shown in bars are absolute numbers of patients.

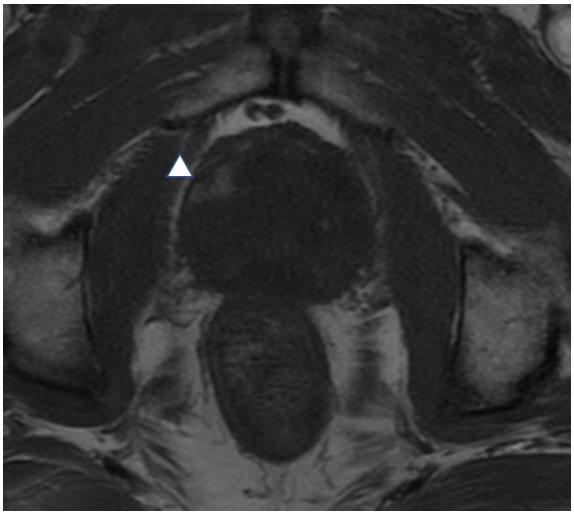

a

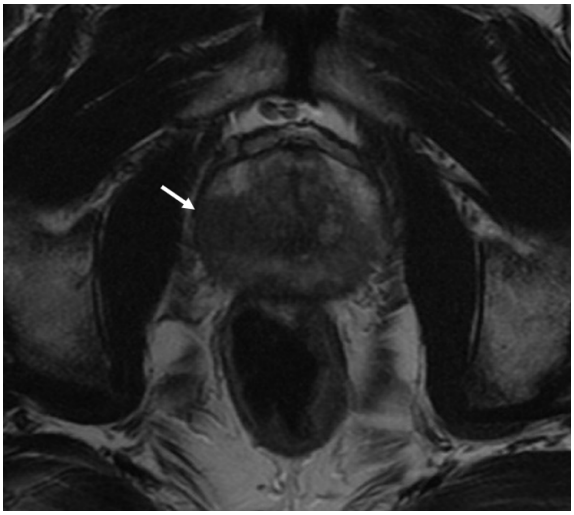

b

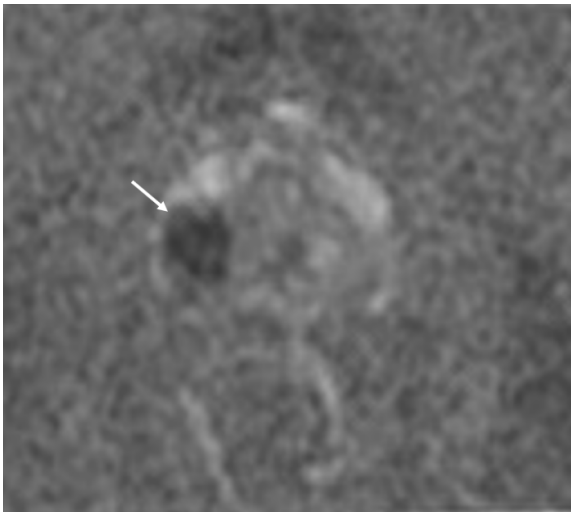

c

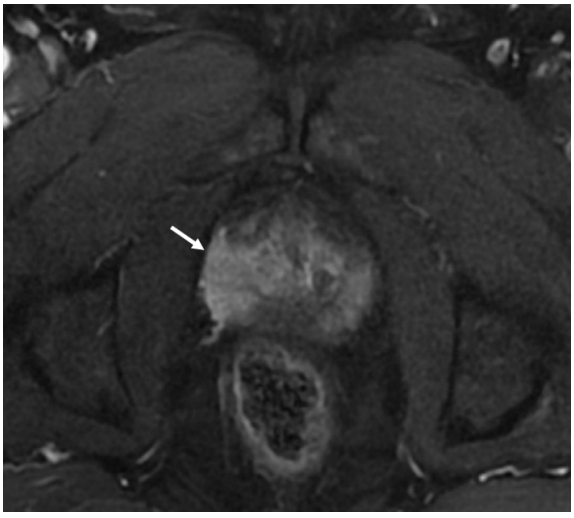

d

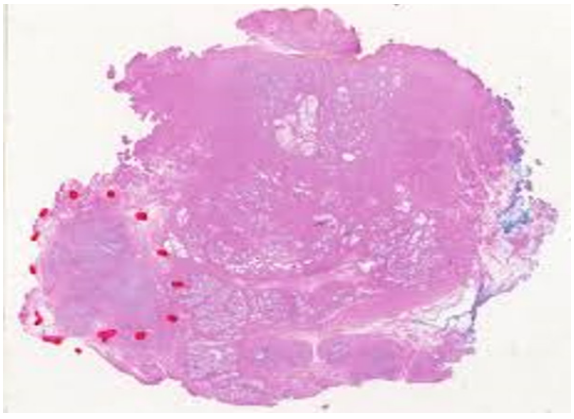

e

Fig. 3. Axial MRI obtained after prostate biopsy in 65-year-old man with prostate specific antigen level of 10.2 ng/mL and positive transrectal biopsy results, indicative of Gleason score of 8 in medial right region of the peripheral zone. (a) T1W MRI shows post-biopsy hemorrhage (arrowhead) as high-signal-intensity areas in PZ. (b) T2W MRI shows a low signal intensity areas (arrow) in right mid-gland of peripheral zone. (c) DW MRI shows a restricted diffusion on apparent diffusion coefficient map (arrow). (d) DCE MRI shows early enhancement (arrow). Standard reading was "No EPE", and specialized reading was "High-grade suspicion of EPE". (e) Whole-mount step-section histopathology found extraprostatic extension at right mid-gland.

analysis for each category of the classification system for the standard and specialized readings. As seen in Figure 2, the AUC for the specialized readings was statistically significantly higher than that for standard readings (0.83 vs. 0.67; P = 0.01). There was a significant correlation between EPE and total hemorrhage score ($r = -0.31$ and $P < 0.01$ for standard reading; $r = -0.26$ and $P < 0.01$ for specialized reading). Figure 3 shows an image example.

DISCUSSION

Our results found that specialized readings by experienced genitourinary radiologist of prostate MRI images with biopsy-related hemorrhage had superior diagnostic performance for the assessment of EPE compared with standard readings. The biopsy-related extensive hemorrhage was identified on T1W imaging in 37% of the patients, and these results were highly reproducible between standard and specialized readings.

The accuracy of the specialized readings was similar to the accuracy reported in the literature for the diagnosis of EPE on MRI (15-17). The differences in diagnostic precision between standard and specialized readings persisted after adjustment for differences in radiologist experience. Recent studies found that the use of MRI results changed the initial surgical strategy for 27% of patients undergoing RP and that the nerve-sparing approach became an option for 61% of these patients (18). Similarly, other studies have found that the use of MRI altered the surgical strategy for 44% of patients studied. Another study found that in 67% of the patients for whom the surgical strategy was altered, a nerve-sparing approach was chosen, and the histopathology suggested that this change was appropriate in each patient (19). The authors concluded that MRI appeared to be "very useful" for identifying candidates for nerve-sparing RP.

Our results showed that the diagnosis of EPE could be affected by post-biopsy hemorrhage. The biopsy-related hemorrhage can disseminate through the ductal system and occupy a larger portion of the prostate gland than would be expected based upon biopsy needle trajectory alone, involving the entire prostate gland in some patients. The presence of hemorrhage poses a major challenge for the diagnoses of EPE with MRI, as blood products can appear as low signal intensity on T2W imaging, thereby obscuring the presence of EPE (20, 21). It has therefore become standard practice to impose a time delay between biopsy and MRI, but this delay can heighten the concern of patients and referring clinicians.

Accurate diagnosis of EPE is generally known to depend on the experience level of the radiologist. We created four diagnostic categories to evaluate sensitivity and specificity for the diagnosis of EPE. When using these categories, the specificity improved, and the sensitivity decreased. However, clinicians will potentially prefer to adopt strict categories to increase degrees of specificity for the diagnosis of EPE. A reverse correlation was identified between EPE and total hemorrhage score. Despite this correlation, there was considerable overlap in the diagnostic accuracy for EPE in patients with post-biopsy hemorrhage.

Our results further expand on results from previous studies assessing the effect of dedicated training and experience on the assessment of EPE by MRI. One study found a clear association between dedicated training and improved accuracy in the diagnosis of EPE on MRI (22). Another study found that for the diagnosis of EPE on MRI, the AUROC for a radiologist with 1.25 years of experience was 0.66, compared to 0.77 for a radiologist with 12 years of experience (23). Although those studies were designed as experimental agreement studies, our study assessed MRI readings from consecutive patients in routine clinical practice. Our results confirm that the reinterpretation of standard reading in MRI by experienced genitourinary radiologists is beneficial for diagnostic performance in the clinical setting. This study provides a scientific justification for this practice and might encourage clinicians to seek a second-opinion reading by subspecialized radiologists. In our study, the accuracy of a standard MRI reading alone was at the lower end of the spectrum, whereas the specialized reading performed exceedingly well. Our results found that the main difference was in sensitivity (44% vs. 75%), while the specificity (87% vs. 84%) was comparable. A "negative" interpretation on standard reading had a higher probability for false-diagnosis of EPE, while the specialized reading reduced this likelihood. A well-established training system that leads to better urologist decisions and management is becoming increasingly important.

Our study had several limitations. First, as with all retrospective studies, there is a risk of selection bias when the treating physician orders the MRI for the purpose of surgery planning. The effect of previous biopsy-related hemorrhage may be somewhat different in a prospective clinical setting. Second, for both the MRI readings and the reference standards, we chose only those patients who underwent prostatectomy, which may have introduced a verification bias in our results. Third, endorectal coil was

not used, which also may have impacted the sensitivity for the diagnosis of EPE. Nevertheless, the use of body surface coils in evaluating EPE is generally recognized in most centers. Finally, because the main purpose of our study was to assess the diagnosis of EPE on a per-patient basis it did not include comparison between every cancer region identified at MRI and histopathology. It is possible that a per-lesion analysis would have shown different results. However, a per-patient analysis has been demonstrated to be acceptable for assessing EPE.

In conclusion, our results demonstrate that even in the presence of post-biopsy hemorrhage, the reinterpretation of MRI images by experienced urogenital radiologists significantly improves the diagnosis of EPE in prostate cancer.

REFERENCES

1. Sciarra A, Barentsz J, Bjartell A, et al. Advances in magnetic resonance imaging: how they are changing the management of prostate cancer. Eur Urol 2011;59:962-977
2. Eberhardt SC, Carter S, Casalino DD, et al. ACR Appropriateness Criteria prostate cancer--pretreatment detection, staging, and surveillance. J Am Coll Radiol 2013;10:83-92
3. Tollefson MK, Karnes RJ, Rangel LJ, Bergstralh EJ, Boorjian SA. The impact of clinical stage on prostate cancer survival following radical prostatectomy. J Urol 2013;189:1707-1712
4. Boccon-Gibod L, Bertaccini A, Bono AV, et al. Management of locally advanced prostate cancer: a European consensus. Int J Clin Pract 2003;57:187-194
5. Yamada AH, Lieskovsky G, Petrovich Z, Chen SC, Groshen S, Skinner DG. Results of radical prostatectomy and adjuvant therapy in the management of locally advanced, clinical stage TC, prostate cancer. Am J Clin Oncol 1994;17:277-285
6. Barrett T, Vargas HA, Akin O, Goldman DA, Hricak H. Value of the hemorrhage exclusion sign on T1-weighted prostate MR images for the detection of prostate cancer. Radiology 2012;263:751-757
7. Rosenkrantz AB, Kopec M, Kong X, et al. Prostate cancer vs. post-biopsy hemorrhage: diagnosis with T2- and diffusion-weighted imaging. J Magn Reson Imaging 2010;31:1387-1394
8. Futterer JJ, Heijmink SW, Scheenen TW, et al. Prostate cancer: local staging at 3-T endorectal MR imaging--early experience. Radiology 2006;238:184-191
9. Pepe P, Dibenedetto G, Garufi A, Priolo G, Pennisi M. Multiparametric pelvic MRI accuracy in diagnosing clinically significant prostate cancer in the reevaluation of biopsy microfocal tumor. Anticancer Res 2015;35:395-399
10. Dickinson L, Ahmed HU, Allen C, et al. Magnetic resonance imaging for the detection, localisation, and characterisation of prostate cancer: recommendations from a European consensus meeting. Eur Urol 2011;59:477-494
11. Quon J, Kielar AZ, Jain R, Schieda N. Assessing the utilization of functional imaging in multiparametric prostate MRI in routine clinical practice. Clin Radiol 2015;70:373-378
12. Magi-Galluzzi C, Evans AJ, Delahunt B, et al. International Society of Urological Pathology (ISUP) Consensus Conference on Handling and Staging of Radical Prostatectomy Specimens. Working group 3: extraprostatic extension, lymphovascular invasion and locally advanced disease. Mod Pathol 2011;24:26-38
13. Samaratunga H, Montironi R, True L, et al. International Society of Urological Pathology (ISUP) Consensus Conference on Handling and Staging of Radical Prostatectomy Specimens. Working group 1: specimen handling. Mod Pathol 2011;24:6-15
14. DeLong ER, DeLong DM, Clarke-Pearson DL. Comparing the areas under two or more correlated receiver operating characteristic curves: a nonparametric approach. Biometrics 1988;44:837-845
15. McClure TD, Margolis DJ, Reiter RE, et al. Use of MR imaging to determine preservation of the neurovascular bundles at robotic-assisted laparoscopic prostatectomy. Radiology 2012;262:874-883
16. Labanaris AP, Zugor V, Takriti S, et al. The role of conventional and functional endorectal magnetic resonance imaging in the decision of whether to preserve or resect the neurovascular bundles during radical retropubic prostatectomy. Scand J Urol Nephrol 2009;43:25-31
17. Akin O, Riedl CC, Ishill NM, Moskowitz CS, Zhang J, Hricak H. Interactive dedicated training curriculum improves accuracy in the interpretation of MR imaging of prostate cancer. Eur Radiol 2010;20:995-1002
18. Futterer JJ, Engelbrecht MR, Huisman HJ, et al. Staging prostate cancer with dynamic contrast-enhanced endorectal MR imaging prior to radical prostatectomy: experienced versus less experienced readers. Radiology 2005;237:541-549
19. Hegde JV, Chen MH, Mulkern RV, Fennessy FM, D'Amico AV, Tempany CM. Preoperative 3-tesla multiparametric endorectal magnetic resonance imaging findings and the odds of upgrading and upstaging at radical prostatectomy

in men with clinically localized prostate cancer. Int J Radiat Oncol Biol Phys 2013;85:e101-107
20. Billing A, Buchner A, Stief C, Roosen A. Preoperative mp-MRI of the prostate provides little information about staging of prostate carcinoma in daily clinical practice. World J Urol 2015;33:923-928
21. Feng TS, Sharif-Afshar AR, Smith SC, et al. Multiparametric magnetic resonance imaging localizes established extracapsular extension of prostate cancer. Urol Oncol 2015;33:109 e115-122
22. Engelbrecht MR, Jager GJ, Laheij RJ, Verbeek AL, van Lier HJ, Barentsz JO. Local staging of prostate cancer using magnetic resonance imaging: a meta-analysis. Eur Radiol 2002;12:2294-2302
23. Woo SM, Kwon TK. Jaceosidin induces apoptosis through Bax activation and down-regulation of Mcl-1 and c-FLIP expression in human renal carcinoma Caki cells. Chem Biol Interact 2016;260:168-175